Journal of
Composites Science

MDPI

Article

EIS Behavior of Polyethylene + Graphite Composite Considered as an Approximation to an Ensemble of Microelectrodes

Javier Navarro-Laboulais [1], José Juan García-Jareño [2], Jerónimo Agrisuelas [2] and Francisco Vicente [2,*]

[1] Instituto Universitario de Seguridad Industrial, Radiofísica y Medioambiental (ISIRYM), Department of Chemical and Nuclear Engineering, Universitat Politècnica de València, Camino de Vera s/n, 46022 València, Spain; jnavarla@iqn.upv.es
[2] Laboratory of Electrochemistry, Department of Physical Chemistry, University of Valencia, C./Dr. Moliner, 50, 46100 Burjassot, Spain; jose.j.garcia@uv.es (J.J.G.-J.); jeronimo.agrisuelas@uv.es (J.A.)
* Correspondence: francisco.vicente@uv.es

Abstract: The electrical percolation of alternating current through two-phase polyethylene/graphite composite electrodes with different contents of graphite microparticles immersed in aqueous KCl solutions has been studied. Above the graphite content of the first percolation threshold, the electrochemical impedance response of this electrode is associated with an equivalent circuit of resistance R_u in series with a constant phase element (CPE). An insulator material + conducting filler model is proposed in which the electroactive surface is considered as the intersection of the percolation cluster through the solid and the cluster associated with the interfacial region. CPE is analyzed assuming a distribution of microcapacitors of the graphite particles in contact with the dielectric solution and inside the dielectric polymeric phase.

Keywords: percolation; fractal dimensions; EIS; CPE; polyethylene/graphite composite

Citation: Navarro-Laboulais, J.; García-Jareño, J.J.; Agrisuelas, J.; Vicente, F. EIS Behavior of Polyethylene + Graphite Composite Considered as an Approximation to an Ensemble of Microelectrodes. *J. Compos. Sci.* **2024**, *8*, 378. https://doi.org/10.3390/jcs8090378

Academic Editor: Hu Liu

Received: 30 July 2024
Revised: 10 September 2024
Accepted: 18 September 2024
Published: 22 September 2024

1. Introduction

Most organic coatings and plastics are composites containing some kind of inorganic filler. Their formulations depend on the chemical–physical properties required in their respective specific applications. Often, a common research topic for their design and development is to predict how the filler ratio in the polymer matrix is affected by possible environmental perturbations on these materials. Technological composites based on polymeric materials reinforced with carbon particles or fibers have been increasingly studied for a long time using electrochemical techniques from a variety of perspectives [1–20]. As a result, they are also increasingly used in the manufacture of electrodes and membranes for conventional electrochemical cells and reactors as well as in everyday electronic devices such as smart phones or personal computers. EIS is an experimental tool for obtaining morphological information about the inside of the material and its surface. This has been very useful in the inhibition of corrosion processes in metals, studies of biomaterials and the development of energy storage devices, as well as the development of sensors or the production of building materials, paints, enamels and varnishes with specific properties.

Historically, the first conductive composites were made by dispersing micrometric conductive particles in insulating polymer matrices. Today, the number of possible benefits and applications of composites of the polymer + conductive charge type has increased enormously, but it should be noted that the theoretical concepts of percolation theory, developed mainly in electrochemical fields during the 20th century [21–34], are still useful to contribute to the design of supercapacitors, electrochemical reactors or sensors, as well as special paints in which these composite materials are used. The surface modification of organic electrodes such as graphite with heteroatoms of high electronegativity is a topic of great technological importance for the development of electrochemical energy storage systems [35].

A seemingly simple model of an insulating polymer + conductive composite is the system consisting of graphite particles dispersed in a polyethylene matrix. Both materials are of great technological importance in their own right. In this work, alternating current is used to characterize the composite material in a conventional three-electrode cell. An attempt is made to obtain information on the effect of the graphite content on the percolation of electric current through it. The electrochemical impedance response of the composite electrode/KCl aqueous solution system is analyzed in order to correlate its surface properties with those of the solid composite and the interfacial regions. This work focuses on the impedance spectroscopy response EIS of the graphite + high-density polyethylene (GHDPE) bicomponent system [36–44]. An attempt is made to correlate the concepts of percolation theory with their phenomenological electrochemical behavior.

For diffusion controlled chronoamperometric processes, it is widely accepted that [30,45–49]

$$j(t) = \sigma_F . t^{-\frac{d_F - 1}{2}} \quad (1)$$

where σ_F is a constant. Then, from the point of view of electrochemical kinetics, the deviation of the ½ value of the exponent of Cottrell's law of Faradaic processes depends on the fractal dimension of its electrode surface and, therefore, also on the experimental ohmic drop of the cell. Consequently, by applying a potential ramp, for example, one could obtain these fractal dimension values from the dependence of the peak intensity of the voltammograms on the scanning rate $\mathbf{v}$, because j_p would be analogously proportional to $\mathbf{v}^{-\frac{d_F - 1}{2}}$ [39,50–52]. In this way, the experimental fractal dimension could be considered as a characteristic measure of the morphology of the surface [53,54]. This fractal dimension is generally associated with surface roughness [55,56].

Since linear scanning cyclic voltammetry, chronoamperometry, and EIS are widely used in laboratories, the calculated values of d_F by means of these classical electrochemical techniques could be of immense practical usefulness for the design and quality control of composite materials in electrochemical devices where electrochemical reactions occur. However, the material transfer processes, passivation and other chemical physical processes as well as secondary chemical reactions coupled with the electron transfer steps can complicate understand the physical meaning of the calculated d_F values.

It is well known that polyethylene is a good non-conductive polymer model and graphite is also a conductive filler model used in technological applications. The dispersion of conductive graphite particles in the non-conductive polyethylene plastic material above the volume content v_C of the percolation threshold produces a multi-microelectrode ensemble on the surface of the electrode composite. The aim of this work is to analyze the electrical percolation through graphite + polyethylene of high-density (GHDPE) electrodes by electrochemical impedance spectroscopy (EIS). The aim is to analyze the fractal dimension of the electrode surfaces of this biphasic composite in the absence of significant faradaic processes, since this electrochemical technique provides direct information on the electrical properties of the material together with the electrode/solution interfaces [36–40,57].

The electrochemical processes should take place at the interface formed between the graphite particles on the composite surface and the aqueous solution of the cell. Obviously, the geometric surface area A_o is not equal to the electroactive area A_{eq} of the electrode. In any case, the fractal dimension of the electrochemical surface d_F is a function of the content of conductive filler into the solid but also depends on the interfacial region. In this scheme, the electrode surface could be considered as the intersection of two percolating clusters: on the one hand, the cluster defined by the transport of electrons through the composite (composite cluster) with a fractal dimension d_C and, on the other hand, the cluster in the interfacial region, which could be defined by means of the lines of force of the charge transfer in the absence of convection (interfacial cluster) d_{DL}. Voltammetry provides rapid information about this electrode process and on the fractal dimension $d_F \cong \mathbf{1.7}$ or the effect of the ohmic drop [37,38]. Although some approximations are required for its calculation [39], the dependence of the electroactive area A_{eq} on the volume fraction of

graphite is consistent with the geometric calculation in the case of a composite of this type [36]. However, the kinetic complications themselves and the overlap between the faradaic and capacitive response introduce an uncertainty in the interpretation of the results. A possible advantage could be to perturb the composite electrodes with an alternating potential using the EIS technique in the absence of electroactive substances in solution in order to simplify the system under study.

2. Materials and Methods

KCl (Aldrich-Sigma; 99%, Madrid, Spain) and $K_3Fe(CN)_6$ (Panreac, Castellar del Vallés, Barcelona, Spain) 99%) have been used as electrolytes solutions. The polymer matrix used to produce these composite materials is a high-density polyethylene (HDPE, Alcudia, REPSOL S.A., Puertollano, Spain) grade. Graphite (Merck 4020, Madrid, Spain) of 16.2 ± 0.2 μm average diameter from the size distribution of the powder particles was used. Experiments using cyclic voltammetry (see Figure S1 in the Supplementary Materials for more information) and EIS were carried out as in previous works by means of a PAR 273A (EG&G) potentiostat/galvanostat [3,36–40] and a AUTOLAB PGSTAB 302 (Metrhom AG, Herisau, Switzerland). In all experiments, a Ag/AgCl/KCl(sat.) reference electrode was used (Metrohm AG, Herisau, Switzerland). DC resistance measurements of work electrodes were made also with a Fluke Mod 45 DC multimeter (Fortive Corporation, NYSE:DHR, Everett, WA, USA, EE. UU.). A conventional double-walled three-electrode cell was used at 298 ± 1 K. We used the following steps to produce electrodes with different amounts of graphite. (1) Mix with a roller mill. (2) Cold crush with a blade mill. (3) Press in a hot plate press. (4) Cut using a diamond saw. The electrodes were made in the form of square prisms 1.0 cm high with square bases of 0.4 cm × 0.6 cm, (see Manufacturing Process in Supplementary Materials); one of the faces was covered with silver paint (Quick Dry Colloidal Silver A 1208, Biorad, Hercules, California, EE. UU.), and for the other, the electrode surface was polished with 600 sandpaper. The electrodes were mounted and embedded in epoxy resin. To confirm the nominal graphite content, the amount of graphite is measured experimentally by thermogravimetric analysis (TGA) at the AIMPLAS Plastics Technological Institute (Paterna, Spain). This is achieved by subjecting the GHDPE sample to 640 °C in an inert atmosphere (N_2 or Ar), which is a temperature at which the polymer matrix breaks down. The volume content of graphite v [3] has been calculated from its weight content m_g and the densities of polyethylene ρ_{PE} and graphite ρ_g:

$$v = \frac{\frac{m_g}{\rho_g}}{\frac{m_g}{\rho_g} + \frac{(1-m_g)}{\rho_{PE}}} \quad (2)$$

From experimental measures of the dependence of the resistance on graphite content, values v_C = 0.14 and t = 3.4 are calculated. Below this critical percolation volume, the composite material shows a resistive behavior (see Figure S2 in Supplementary Materials).

3. Results

3.1. A Fractal Perspective of the EIS of GHDPE/KCl Aqueous Solution Composite

The interfacial region is formed when the electrical circuit in the cell is closed and then, the electrochemical potential gradient associated with charge migration remains generally normal to the electrode surface. Therefore, the fractal dimension (d_F) of the electrode surface must be of the same order as that calculated by the Cotrell equation for diffusion-controlled processes. In the limiting case, the fractal dimension of the electrode surface would approximate the Euclidean dimension $d_F \approx 2$ for a well-polished metallic electrode.

Our hypothesis is that the d_F of the electrode/solution surface is associated with the intersection of two transport clusters (Figure 1). One corresponds to the flow of electrons through the internal cluster of the condensed composite material fractal dimension (d_C), and the other corresponds to the ion transport of the formation of the interfacial region (double layer). The electrochemical surface is the intersection of the composite percolative

cluster with the interfacial cluster formed by the vectorial gradients of the electrochemical potentials at the interfacial region.

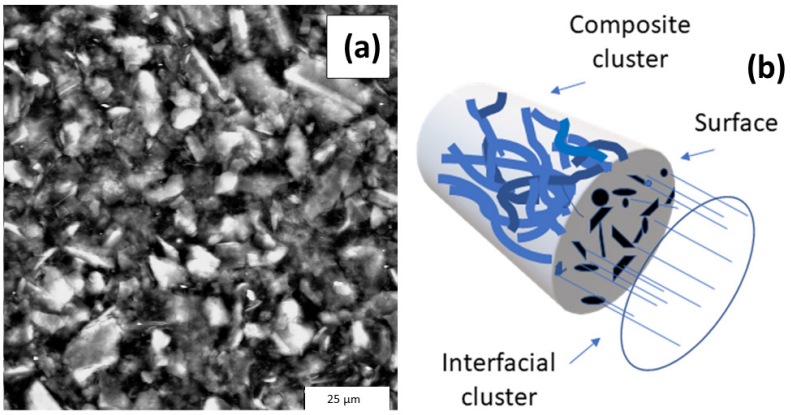

Figure 1. Surface of the composite. (**a**) The surface of GHDPE electrode by SEM with 35% graphite by weight. The bar in the lower right margin represents 25 µm. (**b**) Schematic 3D representation of a cylindrical sample of the composite material of GHDPE electrode.

Therefore, the fractal dimension d_F of the surface electrode is defined as the intersection of a 2D plane embedded in a 3D object $d_E = 3$ [58] as well as the electrode under investigation:

$$d_F = d_C + 2 - d_E = d_C + 2 - 3 = d_C - 1 \quad (3)$$

The fractal dimension of the polymer + graphite composite, d_C, depends increasingly on the probability of occupancy of the particles in the material, p, as a function of their volume content. v (Figure 2). Therefore, in accordance with Equation (3), the fractal dimension of the fractal dimension of the electrode surface d_F should increase with graphite content to a value close to 2.

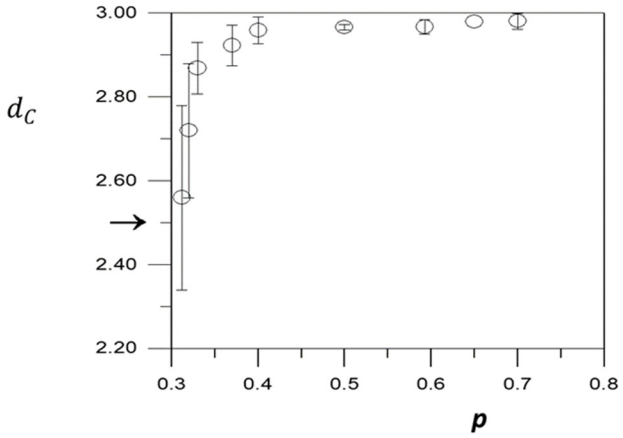

Figure 2. Theorical determination of the fractal dimension of percolation aggregates d_C as a function of the probability of occupation, p. The fractal dimension has been determined by the box-counting method. The arrow on the graph indicates the theoretical value. The error bars have been calculated as the standard deviation of various realizations. It can be seen that the data dispersion follows a law of similarity.

A modulated AC perturbation of the composite-solution system enables obtaining valuable information about the electrical percolation through the system at each stabilization potential E_0 and applied frequency ω. It is generally accepted that the AC current flows through the composite material of the working electrode in three different ways:

polarization, tunneling and directly by electron hopping through the clusters formed by the conductive particles in contact.

By perturbing the dissolution/electrode system with an applied potential at a given frequency ($\omega = 2\pi f$),

$$E(\omega, t) = E_0 + \Delta E\, sin(\omega t) \tag{4}$$

the modulated linear electrochemical response is out of phase in time with a phase angle ($\boldsymbol{\varphi}$) corresponding to the sinusoidal intensity function:

$$\mathrm{i}(\omega, \mathrm{t}) = \mathrm{i}_0 + \Delta \mathrm{i}\, \cos(\omega \mathrm{t} + \varphi) \tag{5}$$

Immediately, it can be concluded that the measure of the phase angle indicates the nature of the percolation of the AC perturbation through the material: $\boldsymbol{\varphi}$ decreases from a limit value of $\pi/2$ rad in the absence of graphite to values typical of a resistive behavior when the content of conductive particles is greater than the first percolation threshold [40]. This implies that the impedance transfer function $Z(\omega) = E(\omega, t)/i(\omega, t)$ provides information about the conductivity of the composite material and the permittivity $\boldsymbol{\varepsilon}$ of the interface. Both electrical quantities then depend on the volume content of graphite $\boldsymbol{v}$. The dependencies of the real and imaginary components of the impedance therefore provide interesting direct information about the system (Figure 3). However, the electrochemical processes that occur in the presence of electroactive substances, including the presence of oxygen in the solution, complicate the interpretation of the electrochemical impedance of the system (Figure S3, results shown as Supplementary Material).

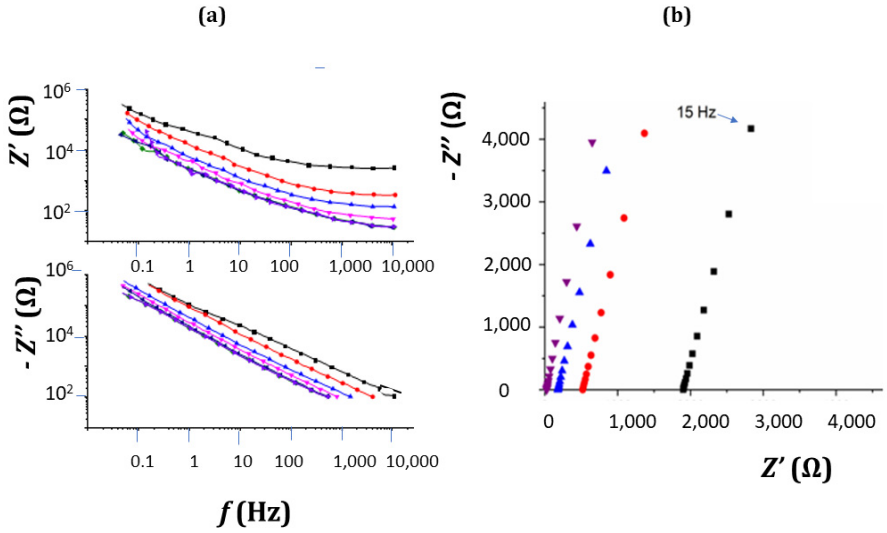

Figure 3. Some EIS spectra. (**a**) Bode plots showing the dependence of the real Z' and imaginary Z'' components on frequency for composite electrode samples of different graphite content **v**: 0.185 (black), 0.229 (red), 0.267 (blue), 0.308 (pink), 0.356 (purple). (**b**) Nyquist plots showing $-Z''$ versus Z''. $E_0 = -0.4$ V; $\Delta E = 10$ mV; 1 M KCl in absence of oxygen; T = 298 K.

The experimental values are fitted to a simple equivalent circuit R-CPE:

$$Z = R_u + (jwq)^{-n} = R_u + Q(jw)^{-n} = R_u + q^{-n}(jw)^{-n} \tag{6}$$

where $j = \sqrt{-1}$, and $\boldsymbol{R_u}$ is the value of the ohmic drop across the cell, which is negligible compared to that of the composite material, while $\boldsymbol{Q}$ and $\boldsymbol{n}$ are fitting coefficients of the real $\mathbf{Z}'$ and imaginary $\mathbf{Z}''$ of the impedance:

$$Z' = Re(Z) = \frac{cos\left(n\frac{\pi}{2}\right)}{(q\omega)^n} + R_u \tag{7}$$

$$Z'' = \mathrm{Im}\,(Z) = \frac{j\,sin\,\left(n\frac{\pi}{2}\right)}{(q\omega)^n} \tag{8}$$

The fractal dimension is related to this exponent, but it depends on the geometry of the cell and its elements [54] and the electrode model considered as well as the particular electrode process. In any case, d_F must be related to the CPE exponent n, which is due to the existence of a time constants distribution on the electroactive surface, as is generally accepted [59–61]. Although the subject is extremely complex, a simple relationship could be postulated as a first approximation to the problem for a planar polished electrode and if it is sufficiently distant from another parallel plane counter-electrode:

$$n = d_{DL} = d_F + 2 - d_E = d_F + 2 - 3 = d_F - 1 \tag{9}$$

In this case, the electrode surface was placed horizontally to avoid gravitational convection. A platinum foil placed parallel to the working electrode was also used as an auxiliary electrode. In this case, the fractal dimension of the cluster was formed by the lines of force in the interfacial region, which is a monodirectional migration transport, $d_{DL} = n \leq 1$.

From another perspective, the interfacial region can be modelized as a framework of graphite particles in contact with the solution in a 2D surface of a geometrical d_F fractal dimension. Also, this interfacial region can be modelized by means an electrical framework of microcapacitors of an overall $C_{DL} \simeq Q = (q^{-n})$, because above the percolation threshold v_C = 0.14, the values of n are close to unity.

Assuming that the electrode surface consists of squares, whose minimum size is $(\delta_0)^2$ and maximum A_0, and assuming that the double-layer capacities C_λ associated with the electrode/dissolution interface are proportional to the number of graphite particles on the surface and their occupied area N_λ, the fractality of the electrode surface can be expressed as follows according to the scaling unit λ (an arbitrary value of area):

$$\left(q^{-n}\right)_\lambda = Q = C_\lambda \cdot N_\lambda = C_\lambda \left(\frac{C_{max}}{C_\lambda}\right)^{d_F} \propto {C_\lambda}^{(1-d_F)} \tag{10}$$

It can be inferred that $n = d_F - 1$, which is the same as

$$d_F = n + 1 \tag{11}$$

As the capacitance is an extensive magnitude proportional to the surface area, it is easy to induce Equation (11), since d_F = 2 and n = 1 in the limit case of an ideal polished electrode surface. However, this hypothesis is quite controversial and represents a drastic approach proposed for this particular model under study. In fact, the correlation between the fractal dimension of fractal electrodes with the exponent of the CPE has been rigorously considered for different electrode models in the literature (Table 1).

Table 1. Some referred dependences of the n on the d_F.

Equations	Conditions	References
$n = 1$	Capacitor	
$n = 0.5$	Warburg	
$n = 0$	Resistance	
$n = -1$	Inductor	
$n = \frac{1}{d_F - 1}$	$2 < d_F < 3$ Porous or rough electrode surface	[48]
$n = \frac{1}{d_F}$	Koch curve and porous/dendritic electrodes	[21,54,62,63]
$n = 3 - d_F$	3D Cantor-bar model	[64,65]
$n = \frac{d_F - 1}{2}$	EIS in diffusive control	[49,66–79]
$n = d_F - 1$	Plane ensemble of micro electrodes	This work

Equation (3) assumes that the interfacial region has an apparent percolative structure formed by the resultant vector of the electrochemical potential gradient, which is considered normal to the plane containing the electroactive graphite particles of the composite surface in contact with the solution. Therefore, the values of d_F are related to the electroactive area occupied A, which is theoretically smaller than the Euclidean geometric one for a well-polished electrode A_O, because the heterogeneous electrode surface is formed by conducting graphite particles dispersed between non-conductive areas of plastic.

In the same ideal way, it is possible to propose a second hypothesis. If we consider that the associated dimensional fractal of the interfacial region depends on the capacitance distribution, analogously in Equation (9), the exponent of the CPE can be considered a fractal dimension of the intersection cluster of the electroactive surface with the cluster of electric charges of the plane-parallel equivalent capacitor, which are both embedded in a raised 3D space. This assumption considers that the capacitance associated with the interfacial region Q is the magnitude of the experimental observation. The physical objects [58] considered fractal are defined as fractal geometric objects in a range [λ_{min}, λ_{max}]. The number of elements N_λ of a range is proportional to λ^{-d_F}:

$$N_\lambda = \left[\frac{\lambda_{max}}{\lambda}\right]^{d_F}, \tag{12}$$

but the concept can be extended to capacitance quantities. If it is accepted that there are a number of squares on the electrode surface N_λ

$$N_\lambda = \left[\frac{q_{\lambda max}}{q_\lambda}\right]^{d_F} \tag{13}$$

contributing to the experimental capacitance in each range of graphite content in the composite analogously to the equation, the following will be fulfilled:

$$Q = q^{-n} = q_\lambda \left[\frac{q_{\lambda max}}{q_\lambda}\right]^{d_F} \propto q_\lambda^{(1-d_F)} \tag{14}$$

It follows Equation (9).

From this perspective, the fractal dimension of the interfacial region is that of the cluster associated with the electrochemical potential gradients normal to the electrode surface: $d_{DL} = n$. This means that by adjusting the impedance measurements to an equivalent circuit consisting of a resistance in series with the CPE, it is possible to estimate d_F values (Table 2). In the extreme ideal case of a well-polished inert metal electrode, the n exponent would approach unity in accordance with the double-layer model of an ideally polarizable electrode, so the fractal dimension of the electrode surface would coincide with the Euclidean fractal dimension of a surface $d_F \approx 2$. While in the case of the real composite, although the electrode surface is polished, the Q constant of the CPE depends on the area of the electroactive surface fraction as well as the concentration of the electrolyte in the interfacial region. In the electrochemical set-up of the experiments carried out, in the absence of convection, and the counter-electrode being a platinum foil parallel to the working electrode, the fractal dimension of the percolation cluster through the interfacial region is the intersection of the fractal of the surface with this migration transport cluster immersed in 3D of the solution.

Table 2. Values of the fractal dimensions of the composite material d_C and its surface d_F estimated from Equations (11) and (3). $E_0 = -0.4$ V; $\Delta E = 10$ mV; 1 M KCl in absence of oxygen; T = 298 K.

m_g	v	R_u Ω	Q μ F	n	d_F	d_C
0.38	0.157	70,000	1.50	0.68	1.68	2.68
0.41	0.176	8400	2.10	0.85	1.85	2.85
0.45	0.186	1900	3.46	0.86	1.86	2.86
0.50	0.220	520	5.13	0.87	1.87	2.87
0.52	0.250	180	5.90	0.88	1.88	2.88
0.65	0.365	25	7.58	0.90	1.90	2.90

3.2. Relation between the Experimental Imaginary Part of the Impedance and the Fractal Dimensions

Laser diffractometry has been used to measure the size dispersion of graphite particles (Figure 4).

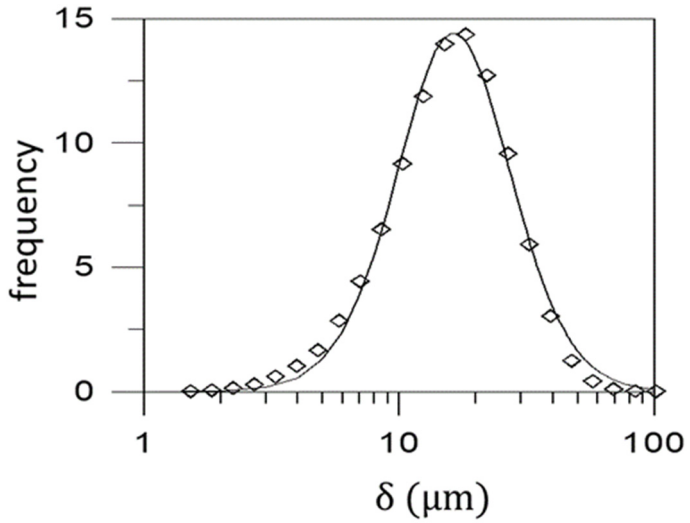

Figure 4. Distribution function of the graphite particles used in the preparation of the composite materials. The line corresponds to a combination of functions obtaining as an average value $\delta_0 = 16.2 \pm 0.2$ μm.

The first percolation threshold $v_C \approx 0.14$ has been calculated from the dependence of the resistance R_u on v measured by dc and EIS (see Figure S2 in the Supplementary Materials). The second percolation threshold corresponds approximately to the volume fraction of graphite at which the material loses its consistency $v_C' \cong 0.41$. Then, the theoretical occupational factor of GHDPE is $\mathbf{f} \approx (0.14 + 0.41) = 0.55$, and the probability of occupation $\mathbf{p_c} \approx 0.254$. This value agrees the theoretical 0.247 ± 0.005 for a percolation of links for a simple cubic structure [58,80,81]. This value is approximately the one obtained by a simulation (Figures 2 and 5). Therefore, the coordination index, $\mathbf{z}$, of a percolation tree is related to the critical threshold by $\mathbf{z} = \mathbf{1}/\mathbf{p_c}$. Substituting the experimental value $\mathbf{p_c} \approx 0.254$, we find for GHDPE that $\mathbf{z} = 3.94 \approx 4$. This value is consistent with the calculated occupancy factor in accordance with the anisotropic conductance of the graphite particles.

EIS provides valuable information in the case of the GHDPE system immersed in an electrolyte dissolution. From the real component of the impedance, extrapolating to infinite frequency, the values of R_u could be calculated. From the module of the imaginary component, the capacitive character of the electrode is extracted.

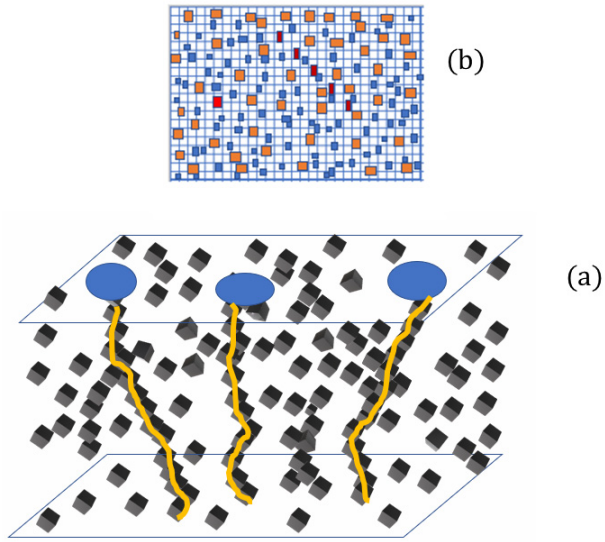

Figure 5. Simulation of the bulk (**a**) and surface electrode (**b**), considering that each graphite particles occupies cubes and squares of sides δ_0 = 16.2 µm, respectively. Only a limited number of surface graphite particles pertain to a conductive cluster (red squares in (**b**)). The white squares represent the surface occupied by polyethylene. The blue squares represent the graphite particles not belonging to a percolative cluster. The overall number of squares of the electrode surface is 92,226. The overall number of cubes of the electrodes samples is approximately 56,444,026. Simulated v_C = 0.154 (3D) and v_C = 0.44 (2D) where calculated.

From the limit at high frequencies of the real impedance component, the resistance R_u is calculated, but in addition, the CPE parameters are calculated as well, which provide information on the distribution of potentials and time constants on the electrode surface, which is directly related to the fractal dimension d_F of the electrode surface. Q increases as the proportion of surface occupied by graphite is greater, which is in agreement with the predictions of the percolation theory and the experimental data obtained by EIS (Figure 6a). The parabolic curve starts from the point corresponding to the percolation threshold $v_C \approx 0.14$ to the theorical maximum capacitance associated with the double layer of the electrode–solution interface $C_{DLA_0} \simeq 51.73$ µF.

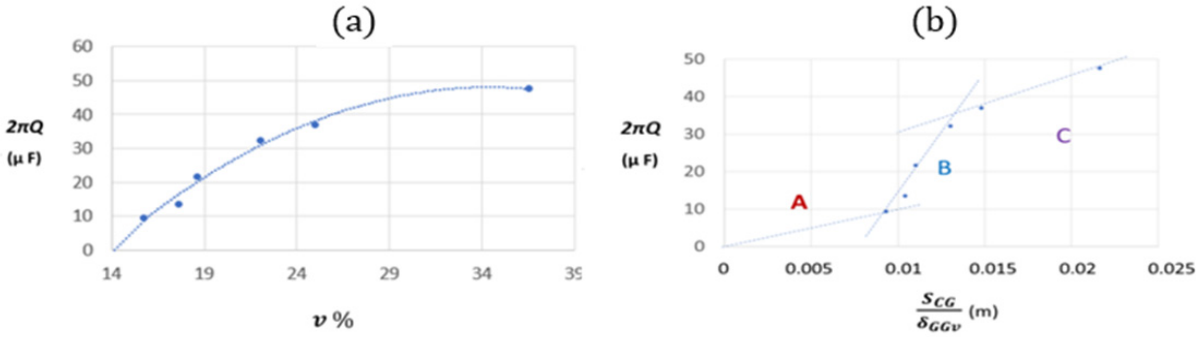

Figure 6. (**a**) Dependence of the Q parameter on the volume percentage of graphite. (**b**) Dependence of the Q parameter on the ratio of the overall electrical active surface of the graphite particles S_{CG} and their separation δ_{GGv}. In A, the surface microcapacitors are separated. In zone B, the graphite particles approach each other. In zone C, the microcapacitors are associated in series. E_0 = 0.4 V; ΔE = 10 mV; 1 M KCl in absence of oxygen; T = 298 K.

From the values of the CPE coefficients for the samples with different contents of conductive filler, two qualitatively different ranges are distinguished over the percolation threshold: a range at which the values of Q and n grow on the graphite content, and another in which both parameters vary little (Table 2 and Figure 6b). Despite the probability of

current passage across the bulk over v_C = 0.14 being P = 1 in both ranges, the potential dispersion at the multi-microelectrodes of the graphite particles on the surface of the composite is less over v = 0.25, showing that the surface reaches a single behavior in the interfacial region because the calculated n remains practically constant (Table 2). These results are consistent with the initial hypothesis that the electrode surface is the result of the intersection of the cluster of the composite with the cluster associated at the perpendicular plane interfacial region. Processes that take place in the interfacial region are based on the fractal modeling of the three-dimensional percolative cluster of the solid composite d_C (see the last column of Table 2) and are close to the theoretically [58] calculated values for an infinite cluster d_C = 2.523.

If the coefficient n has been associated with the fractal dimension of the surface of the electrode, the physical meaning of the constant Q is clear when the parameter n tends to unity. For graphite contents, $v \geq 0.25$, the capacity of the double layer can be considered as corresponding to the equivalent associated capacitors of C_i, which are formed by the individual graphite particles on the surface in contact with the aqueous KCl solution. Therefore, it can be simplified, assuming that the interfacial region shows a phenomenological capacitance that depends on an apparent dielectric permittivity ε of the dissolution and an apparent thickness δ_{DL} of the double layer, which is named the frequently reciprocal Debye length:

$$(C_{DL})_\lambda = \varepsilon A_\lambda / \delta_{DL} \quad (15)$$

where A_λ is the area of a selected electroactive experimental surface of the electrode. Therefore, the value of this parameter can be considered proportional to the fraction of area occupied by the graphite particles located on the surface of the electrode. At low concentrations of KCl, the Debye length varies with the square root of the inverse ionic strength if the interfacial region is considered as an equivalent parallel plate capacitor [82–84].

In accordance with the assumption of Equation (9), the exponent of the CPE can be considered directly as a fractal dimension of the intersection cluster of the electrochemical surface cluster of d_F with the electrical charges of the other capacitor plate of $d_F^{'} \approx 2$, which are both embedded in a 3D space. That justifies the hypothesis embodied in Equation (3) in the simple model proposed where the CPE is directly related to the electrical properties of the interfacial region only. However, if the CPE included in the equivalent circuit is directly associated with the solid electrode as well as the case of deposited films [85] or porous and rough electrodes (Table 2), the interpretation of the constant-phase-element is in general more complicated [40,86,87]. In this composite, the real and imaginary components of the impedance depend on both CPE parameters following Equations (9) and (10). This suggests that the proposed model based on the self-definition of the R-CPE circuit is apparently useful for describing the electrochemical behavior of the composite electrode/solution for graphite contents $v \geq v_C$. However, this hypothesis, which is based on the intuitive idea that the imaginary component of the impedance depends only on the electrode/solution interface, requires further discussion, because the surface morphology of the electrode depends directly on the percolation inside the material. Therefore, in this system, lacking porosity and significant faradaic processes, the CPE associated with the imaginary part must depend on the distribution of graphite particles on the surface and also inside the material. That is, it depends on the particle/solution interfaces at the surface as well as to a large extent on the graphite particle/polyethylene interface inside the material.

4. Discussion

Assuming that the average particle radius is 16 ± 2 μm and the Debye length $\delta_{DL} \simeq 0.3$ nm for a 1 M electrolyte 1:1 solution, and considering that the relative dielectric permeability of the solution $\varepsilon_{KCl1M} \simeq 74$ at room T = 298 K [84], an approximate value of

the double-layer capacitance of the electrode/solution interfacial region (Table 3) can be estimated according to the following equation:

$$C_{DL} = (74)(8.854 \times 10^{-12}\ \mathrm{F.m^{-1}})\ \frac{A}{(0.3 \times 10^{-9}\ \mathrm{m})} \quad (16)$$

Table 3. An estimation of the fraction $\boldsymbol{\theta}$ occupied on the surface of the particles that include DC-conducting clusters. Approximated distances between the graphite particles considered as cubes of δ_0 = 16.2 nm: δ_{GGv}, which occupies an estimated overall area S_{CG} considering **z** = 4. The electroactive area A_{eq} was obtained from a potentiostatic reduction of 1.0 mM of K_3 [Fe(CN)$_6$] in KCl 1 M [40] on composite electrodes of A_0 = 0.24 mm^2 of Euclidean area. T = 298 K. E = −0.4 V vs. Ag/AgCl/KCl (sat.) 1 M KCl.

v ...	Q µ F	S_{CG} m^2	δ_{GGv} µ m	θ	A_{eq} mm^2	τ µ s
0.157	1.50	0.010	27	0.029	0.211	105
0.176	2.10	0.011	26	0.041	0.234	18
0.186	3.46	0.014	24	0.067	0.240	6
0.220	5.13	0.015	23	0.092	0.246	3
0.250	5.90	0.021	20	0.114	0.250	5
0.365	7.58	0.024	18	0.147	0.274	7

Assuming that all N_G particles of graphite

$$N_G = \frac{v}{(16.2)^3}\ (240)10^9 \quad (17)$$

possess this same average size and show four conductive faces to give rise to microcapacitors, it is possible to calculate a total area susceptible to act as an array of graphite/polyethylene interface microcapacitors S_{CG}, whose average spacing is near

$$\delta_{GGv} = \sqrt[3]{\frac{1-v}{v}}\ \delta_0 \quad (18)$$

which decreases as the partial volume of polyethylene decreases.

Here, C_{DL} is the double-layer capacitance associated with all the graphite particles on the surface belonging to conductive clusters that are in contact with the solution (Figure 5b), considering that the fraction of surface area occupied by these particles can calculated as

$$\theta = \frac{Q}{C_{DLA_0}} \quad (19)$$

where $C_{DLA_0} = 51.73$ µF is the double-layer capacitance calculated according to Equation (16) for the 0.24 mm^2 surface area electrode assuming that the entire geometric surface area of the electrode was occupied by conductive particles.

The $\boldsymbol{\theta}$ values in Table 3 assume that not all graphite particles in each plane perpendicular to the current direction participate in the percolative cluster. This is consistent with the fact that the polarization conduction of the alternating current is added to the current conduction of the direct contact and the tunneling effect. This leads to an increase in the electroactive area of the composite electrodes, which is consistent with the relatively high experimental values of the electroactive area in faradaic processes (Table 3).

This involvement of the graphite/polyethylene interfaces in the electrode/dissolution double-layer values would explain the phenomenological behavior of these materials as macroscopic electrodes. Only at ratios close to the percolation threshold (zone A in Figure 6b), when there are few percolating clusters with terminal graphite particles, would the surface microcapacitors be associated in parallel, but as the proportion of graphite increases, the interparticle distance decreases and the total particle area within the material

increases dramatically (zone B in Figure 6b). Also, the distance between the graphite particles on the surface $\delta_{GG}^{\theta} \simeq \sqrt[2]{\frac{1-\theta}{\theta}}\delta_0$ decreases and, consequently, the surface percolation increases (zone C in Figure 6b). Q reaches previsibly the limit of the double-layer capacity C_{DLA_0}. This maximum value is consistent with surface microcapacitors connected in series covering all electroactive surface. For a calculated total area of the graphite particles of less than 0.01 m^2 (ν less than 0.176), the number of graphite particles on the electrode surface belonging to a conductive cluster is very small. In the intermediate zone B, there is a transition from a dispersion of microelectrodes to a content of ν greater than 0.22, which is clearly a macroscopic electrode. One explanation for this transition may be based on the fact that polyethylene has a strong tendency to accumulate charge.

As the number of microparticles increases, the average distance between them decreases, and the composite behaves macroscopically as a homogeneous semiconductor. This can be explained on the basis that when the distance between the particles is of the order of their size, the circuit is short circuited by the interfacial region through the solution.

Looking at the dependence of the characteristic time $\tau \simeq R_u \cdot Q$ with the graphite content, there is a change in trend for values above v = 0.22. Also, it is striking that the values of n are close to those corresponding to a pure capacitor, as if it were a macroelectrode, which is consistent with the relative values of the electroactive area calculated for the faradaic process of reduction of the K_3 [$Fe(CN)_6$], although in the case of an electrochemical reaction controlled by mass transfer on published electrodes, the value of n should be close to ½. This is because in the species, they can move equiprobably by diffusion in two senses, whereas there is only one directional sense of movement of charged particles by the migration imposed by the instantaneous electric field.

In spite of the practical interest of Equations (16)–(19), it is necessary to confirm their accuracy for these and other similar composite materials by means of complementary experimental techniques [88] in different media.

5. Conclusions

The response to the alternating current of the electrode/solution has been analyzed, and a model is proposed in which the fractal dimension of the electrode surface is correlated with the exponent of the CPE, in which the electroactive surface is the intersection of two clusters: that of the solid and that formed by the perpendicular electric fields to the surface. From this perspective, the value of the CPE constant Q is related to the association of microcapacitors that form in the interfacial region between the graphite particles dispersed on the surface of the composite and the solution. This approach is consistent with the fact that the real component of the impedance is directly associated with the fractal dimension of the electrical percolation cluster d_C (3D) through the solid composite, while the imaginary component of the impedance has been associated with the formation of the interfacial region on an electrode surface of fractal dimension d_F (2D), which is consistent with the fact that the exponent n of the CPE could be considered as the fractal dimension d_{DL} (1D) of the interfacial region.

Supplementary Materials: The following supporting information can be downloaded at https://www.mdpi.com/article/10.3390/jcs8090378/s1, Figure S1. The shape of the voltammograms of the electrodes; Manufacturing Process; Figure S2. The resistance measured (DC curve) agrees well with that measured by EIS; Figure S3. Faradaic processes associated with the presence of oxygen in the solution; Figure S4. The total surface area of the particles and their separations depend on the shape and size distribution.

Author Contributions: J.N.-L., J.A., J.J.G.-J. and F.V.: Conceptualization, methodology, validation, formal analysis, resources, data curation, writing—original draft preparation, writing—review and editing, visualization, project administration, funding acquisition. All authors have read and agreed to the published version of the manuscript.

Funding: Thanks to the support of the Spanish Network of Excellence Environmental and Energy Applications of Electrochemical Technology. MICINN/AEI: RED2022-134552-T.

Institutional Review Board Statement: Not applicable.

Informed Consent Statement: Not applicable.

Data Availability Statement: Data available under demand.

Acknowledgments: Thanks to José Trijueque (Technological Institute of Plastics AIMPLAS, Paterna, Spain) for having helped in the manufacture of the composite and in the discussion of results.

Conflicts of Interest: The authors declare no conflicts of interest.

References

1. Lin, L.; Ning, H.; Song, S.; Xu, C.; Hu, N. Flexible Electrochemical Energy Storage: The Role of Composite Materials. *Compos. Sci. Technol.* **2020**, *192*, 108102. [CrossRef]
2. Islam, J.; Chowdhury, F.; Uddin, J.; Amin, R.; Uddin, J. Review on Carbonaceous Materials and Metal Composites in Deformable Electrodes for Flexible Lithium-Ion Batteries. *RSC Adv.* **2021**, *11*, 5958–5992. [CrossRef] [PubMed]
3. Navarro-Laboulais, J.; Trijueque, J.; García-Jareño, J.J.; Vicente, F. Impedance Analysis of Graphite + Polyethylene and Graphite + Epoxy Composite Electrodes. *J. Electroanal. Chem.* **1995**, *399*, 115–120. [CrossRef]
4. Li, G.; Xia, Y.; Tian, Y.; Wu, Y.; Liu, J.; He, Q.; Chen, D. Review—Recent Developments on Graphene-Based Electrochemical Sensors toward Nitrite. *J. Electrochem. Soc.* **2019**, *166*, B881–B895. [CrossRef]
5. Himadri Reddy, P.C.; Amalraj, J.; Ranganatha, S.; Patil, S.S.; Chandrasekaran, S. A Review on Effect of Conducting Polymers on Carbon-Based Electrode Materials for Electrochemical Supercapacitors. *Synth. Met.* **2023**, *298*, 117447. [CrossRef]
6. Gao, X.; Li, W.; Wang, P.; Lu, Y.; Zhou, J.; Wang, X.Q. Advancing Energy Solutions: Carbon-Based Cementitious Composites in Energy Storage and Harvesting. *J. Build. Eng.* **2024**, *91*, 109720. [CrossRef]
7. Das, N.C.; Maiti, S. Electromagnetic Interference Shielding of Carbon Nanotube/Ethylene Vinyl Acetate Composites. *J. Mater. Sci.* **2008**, *43*, 1920–1925. [CrossRef]
8. Miller, E.E.; Hua, Y.; Tezel, F.H. Materials for Energy Storage: Review of Electrode Materials and Methods of Increasing Capacitance for Supercapacitors. *J. Energy Storage* **2018**, *20*, 30–40. [CrossRef]
9. Faga, M.; Duraccio, D.; Di Maro, M.; Pedraza, R.; Bartoli, M.; d'Ayala, G.; Torsello, D.; Ghigo, G.; Malucelli, G. Ethylene-Vinyl Acetate (EVA) Containing Waste Hemp-Derived Biochar Fibers: Mechanical, Electrical, Thermal and Tribological Behavior. *Polymers* **2022**, *14*, 4171. [CrossRef]
10. Fang, H.; Yang, D.; Su, Z.; Sun, X.; Ren, J.; Li, L.; Wang, K. Preparation and Application of Graphene and Derived Carbon Materials in Supercapacitors: A Review. *Coatings* **2022**, *12*, 1312. [CrossRef]
11. Wang, P.; Song, T.; Abo-Dief, H.M.; Song, J.; Alanazi, A.K.; Fan, B.; Huang, M.; Lin, Z.; Altalhi, A.A.; Gao, S.; et al. Effect of Carbon Nanotubes on the Interface Evolution and Dielectric Properties of Polylactic Acid/Ethylene–Vinyl Acetate Copolymer Nanocomposites. *Adv. Compos. Hybrid Mater.* **2022**, *5*, 1100–1110. [CrossRef]
12. Agrisuelas, J.; Balart, R.; García-Jareño, J.J.; López-Martínez, J.; Vicente, F. A Macroscopic Interpretation of the Correlation between Electrical Percolation and Mechanical Properties of Poly-(Ethylene Vinyl Acetate)/Zn Composites. *Materials* **2024**, *17*, 2527. [CrossRef] [PubMed]
13. Vovchenko, L.; Perets, Y.; Ovsienko, I.; Matzui, L.; Oliynyk, V.; Launetz, V. Shielding Coatings Based on Carbon–Polymer Composites. *Surf. Coat. Technol.* **2012**, *211*, 196–199. [CrossRef]
14. Peng, Y.; Burtovyy, R.; Bordia, R.; Luzinov, I. Fabrication of Porous Carbon Films and Their Impact on Carbon/Polypropylene Interfacial Bonding. *J. Compos. Sci.* **2021**, *5*, 108. [CrossRef]
15. Kratofil Krehula, L.; Peršić, A.; Popov, N.; Krehula, S. Polymer Composites of Low-Density Polyethylene (LDPE) with Elongated Hematite (α-Fe_2O_3) Particles of Different Shapes. *J. Compos. Sci.* **2024**, *8*, 73. [CrossRef]
16. Sadeghi, P.; Goli, A.; Fini, E. Carbon Sequestration via Bituminous Composites Containing Recycled High-Density Polyethylene. *J. Compos. Sci.* **2024**, *8*, 100. [CrossRef]
17. Kou, Y.; Cheng, X.; Macosko, C.W. Degradation and Breakdown of Polymer/Graphene Composites under Strong Electric Field. *J. Compos. Sci.* **2022**, *6*, 139. [CrossRef]
18. Gangwani, P.; Kovač, J.; Emami, N.; Kalin, M. Effect of Multi-Scale Fillers on the Tribological Behavior of UHMWPE Composites in Water-Lubricated Contacts. *Tribol. Int.* **2024**, *196*, 109669. [CrossRef]
19. Maniadi, A.; Vamvakaki, M.; Suchea, M.; Tudose, I.V.; Popescu, M.; Romanitan, C.; Pachiu, C.; Ionescu, O.N.; Viskadourakis, Z.; Kenanakis, G.; et al. Effect of Graphene Nanoplatelets on the Structure, the Morphology, and the Dielectric Behavior of Low-Density Polyethylene Nanocomposites. *Materials* **2020**, *13*, 4776. [CrossRef]
20. Olesik, P.; Godzierz, M.; Kozioł, M.; Jała, J.; Szeluga, U.; Myalski, J. Structure and Mechanical Properties of High-Density Polyethylene Composites Reinforced with Glassy Carbon. *Materials* **2021**, *14*, 4024. [CrossRef]
21. Kahanda, G.L.M.K.S.; Tomkiewicz, M. Fractality and Impedance of Electrochemically Grown Silver Deposits. *J. Electrochem. Soc.* **1990**, *137*, 3423. [CrossRef]
22. Sunde, S. Calculation of Conductivity and Polarization Resistance of Composite SOFC Electrodes from Random Resistor Networks. *J. Electrochem. Soc.* **1995**, *142*, L50. [CrossRef]

23. De Arcangelis, L.; Redner, S.; Coniglio, A. Anomalous Voltage Distribution of Random Resistor Networks and a New Model for the Backbone at the Percolation-Threshold. *Phys. Rev. B* **1985**, *31*, 4725–4727. [CrossRef] [PubMed]
24. De Arcangelis, L.; Redner, S.; Coniglio, A. Multiscaling Approach in Random Resistor and Random Superconducting Networks. *Phys. Rev. B* **1986**, *34*, 4656–4673. [CrossRef] [PubMed]
25. Angulo, R.; Medina, E. Conductance Distributions in Random Resistor Networks—Self-Averaging and Disorder Lengths. *J. Stat. Phys.* **1994**, *75*, 135–151. [CrossRef]
26. Koch, D.L.; Sangani, A.S. The AC Electrical Impedance of a Fractal Boundary to an Electrolytic Solution. *J. Electrochem. Soc.* **1991**, *138*, 475. [CrossRef]
27. Lust, L.; Kakalios, J. Computer-Simulations of Conductance Noise in a Dynamical Percolation Resistor Network. *Phys. Rev. E* **1994**, *50*, 3431–3435. [CrossRef]
28. Babalievski, F. Algorithm to Extract the Spanning Clusters and Calculate Conductivity in Strip Geometries. *Phys. Rev. E* **1995**, *51*, 6230–6234. [CrossRef]
29. Kolek, A. Voltage Distribution in a Two-Component Random System. *Phys. Rev. B* **1996**, *53*, 14185–14195. [CrossRef]
30. Batrouni, G.G.; Hansen, A.; Larson, B. Current Distribution in the Three-Dimensional Random Resistor Network at the Percolation Threshold. *Phys. Rev. E* **1996**, *53*, 2292–2297. [CrossRef]
31. Barta, S.; Dieska, P. A Computer-Simulation Study of Anomalous Diffusion on Percolating Clusters Near to the Critical-Point. *Phys. A* **1995**, *215*, 251–260. [CrossRef]
32. Lopez, J.; Rodriguez, M.; Pesquera, L. Analysis of Self-Averaging Properties in the Transport of Particles Through Random-Media. *Phys. Rev. E* **1995**, *51*, R1637–R1640. [CrossRef]
33. Bunde, A.; Havlin, S.; Porto, M. Are Branched Polymers in the Universality Class of Percolation. *Phys. Rev. Lett.* **1995**, *74*, 2714–2716. [CrossRef] [PubMed]
34. Scher, H.; Zallen, R. Critical Density in Percolation Processes. *J. Chem. Phys.* **1970**, *53*, 3759. [CrossRef]
35. Gupta, R.; Malik, A.; Kumari, K.; Singh, S.K.; Vivier, V.; Mondal, P.C. Metal-Free Platforms for Molecular Thin Films as High-Performance Supercapacitors. *Chem. Sci.* **2024**, *15*, 8775–8785. [CrossRef] [PubMed]
36. Navarro-Laboulais, J.; García-Jareño, J.J.; Vicente, F. Kramers–Kronig Transformation, Dc Behaviour and Steady State Response of the Warburg Impedance for a Disk Electrode Inlaid in an Insulating Surface. *J. Electroanal. Chem.* **2002**, *536*, 11–18. [CrossRef]
37. Beaunier, L.; Keddam, M.; Garcia-Jareno, J.J.; Vicente, F.; Navarro-Laboulais, J. Surface Structure Determination by SEM Image Processing and Electrochemical Impedance of Graphite plus Polyethylene Composite Electrodes. *J. Electroanal. Chem.* **2004**, *566*, 159–167. [CrossRef]
38. Navarro-Laboulais, J.; Trijueque, J.; García-Jareño, J.J.; Vicente, F. Ohmic Drop Effect on the Voltammetric Behaviour of Graphite + Polyethylene Composite Electrodes. *J. Electroanal. Chem.* **1997**, *422*, 91–97. [CrossRef]
39. Navarro-Laboulais, J.; Trijueque, J.; García-Jareño, J.J.; Benito, D.; Vicente, F. Determination of the Electroactive Area of Graphite + polyethylene Composite Electrodes. Uncompensated Resistance Effects and Convolution Analysis of Chronoamperograms. *J. Electroanal. Chem.* **1998**, *443*, 41–48. [CrossRef]
40. Navarro-Laboulais, J.; Trijueque, J.; García-Jareño, J.J.; Benito, D.; Vicente, F. Electrochemical Impedance Spectroscopy of Conductor—Insulator Composite Electrodes: Properties in the Blocking and Diffusive Regimes. *J. Electroanal. Chem.* **1998**, *444*, 173–186. [CrossRef]
41. Bhattacharya, S.; Tandon, R.P.; Sachdev, V.K. Electrical Conduction of Graphite Filled High Density Polyethylene Composites; Experiment and Theory. *J. Mater. Sci.* **2009**, *44*, 2430–2433. [CrossRef]
42. Panwar, V.; Mehra, R.M. Analysis of Electrical, Dielectric, and Electromagnetic Interference Shielding Behavior of Graphite Filled High Density Polyethylene Composites. *Polym. Eng. Sci.* **2008**, *48*, 2178–2187. [CrossRef]
43. Luo, W.; Cheng, C.; Zhou, S.; Zou, H.; Liang, M. Thermal, Electrical and Rheological Behavior of High-Density Polyethylene/Graphite Composites. *Iran. Polym. J.* **2015**, *24*, 573–581. [CrossRef]
44. Krupa, I.; Novák, I.; Chodák, I. Electrically and Thermally Conductive Polyethylene/Graphite Composites and Their Mechanical Properties. *Synth. Met.* **2004**, *145*, 245–252. [CrossRef]
45. Agrisuelas, J.; García-Jareño, J.J.; Gimenez-Romero, D.; Negrete, F.; Vicente, F. The Fractal Dimension as Estimator of the Fractional Content of Metal Matrix Composite Materials. *J. Solid State Electrochem.* **2009**, *13*, 1599–1603. [CrossRef]
46. Ghanbari, K.; Mousavi, M.F.; Shamsipur, M.; Rahmanifar, M.S.; Heli, H. Change in Morphology of Polyaniline/Graphite Composite: A Fractal Dimension Approach. *Synth. Met.* **2006**, *156*, 911–916. [CrossRef]
47. Lee, S.-B.; Pyun, S.-I. Determination of the Morphology of Surface Groups Formed and PVDF-Binder Materials Dispersed on Graphite Composite Electrodes in Terms of Fractal Geometry. *J. Electroanal. Chem.* **2003**, *556*, 75–82. [CrossRef]
48. Nyikos, L.; Pajkossy, T. Fractal Dimension and Fractional Power Frequency-Dependent Impedance of Blocking Electrodes. *Electrochim. Acta* **1985**, *30*, 1533–1540. [CrossRef]
49. Dassas, Y.; Duby, P. Diffusion toward Fractal, Interfaces Potentiostatic, Galvanostatic, and Linear Sweep Voltammetric Techniques. *J. Electrochem. Soc.* **1995**, *142*, 4175–4180. [CrossRef]
50. Navarro-Laboulais, J.; Vilaplana, J.; López, J.; García-Jareño, J.J.; Benito, D.; Vicente, F. Prussian Blue Films Deposited on Graphite + epoxy Composite Electrodes: Electrochemical Detection of the Second Percolation Threshold. *J. Electroanal. Chem.* **2000**, *484*, 33–40. [CrossRef]

51. Trijueque, J.; García-Jareño, J.J.; Navarro-Laboulais, J.; Sanmatías, A.; Vicente, F. Ohmic Drop of Prussian-Blue/Graphite + epoxy Electrodes. *Electrochim. Acta* **1999**, *45*, 789–795. [CrossRef]
52. García-Jareño, J.J.; Sanmatías, A.; Navarro-Laboulais, J.; Vicente, F. Chronoamperometry of Prussian Blue Films on ITO Electrodes: Ohmic Drop and Film Thickness Effect. *Electrochim. Acta* **1999**, *44*, 4753–4762. [CrossRef]
53. Pajkossy, T.; Nyikos, L. Scaling-Law Analysis to Describe the Impedance Behavior of Fractal Electrodes. *Phys. Rev. B* **1990**, *42*, 709–719. [CrossRef] [PubMed]
54. Sapoval, B.; Gutfraind, R.; Meakin, P.; Keddam, M.; Takenouti, H. Equivalent-Circuit, Scaling, Random-Walk Simulation, and an Experimental-Study of Self-Similar Fractal Electrodes and Interfaces. *Phys. Rev. E* **1993**, *48*, 3333–3344. [CrossRef] [PubMed]
55. Dobrescu, G.; Georgescu-State, R.; Papa, F.; Staden, J.; Koos, F.V.; State, R.N. Fractal Properties of Composite-Modified Carbon Paste Electrodes—A Comparison between SEM and CV Fractal Analysis. *Fractal Fract.* **2024**, *8*, 205. [CrossRef]
56. Giménez-Romero, D.; García-Jareño, J.J.; Vicente, F. Correlation between the Fractal Dimension of the Electrode Surface and the EIS of the Zinc Anodic Dissolution for Different Kinds of Galvanized Steel. *Electrochem. Commun.* **2004**, *6*, 148–152. [CrossRef]
57. Aoki, K.J. Frequency-Dependence of Electric Double Layer Capacitance without Faradaic Reactions. *J. Electroanal. Chem.* **2016**, *779*, 117–125. [CrossRef]
58. Isichenko, M.B. Percolation, Statistical Topography, and Transport in Random Media. *Rev. Mod. Phys.* **1992**, *64*, 961–1043. [CrossRef]
59. Alexander, C.L.; Tribollet, B.; Orazem, M.E. Contribution of Surface Distributions to Constant-Phase-Element (CPE) Behavior: 2. Capacitance. *Electrochim. Acta* **2016**, *188*, 566–573. [CrossRef]
60. Orazem, M.E.; Tribollet, B.; Vivier, V.; Riemer, D.P.; White, E.; Bunge, A. On the Use of the Power-Law Model for Interpreting Constant-Phase-Element Parameters. *J. Braz. Chem. Soc.* **2014**, *25*, 532–539. [CrossRef]
61. Gateman, S.M.; Gharbi, O.; Gomes De Melo, H.; Ngo, K.; Turmine, M.; Vivier, V. On the Use of a Constant Phase Element (CPE) in Electrochemistry. *Curr. Opin. Electrochem.* **2022**, *36*, 101133. [CrossRef]
62. Jaroniec, M. The Fractal Approach to Heterogeneous Chemistry: Surfaces, Colloids, Polymers. Edited by David Avnir, Wiley, New York. 1989, 311. *AIChE J.* **1990**, *36*, 1456. [CrossRef]
63. Meakin, P.; Sapoval, B. Random-Walk Simulation of the Response of Irregular or Fractal Interfaces and Membranes. *Phys. Rev. A* **1991**, *43*, 2993–3004. [CrossRef] [PubMed]
64. Kaplan, T.; Liu, S.; Gray, L. Inverse-Cantor-Bar Model for the Ac Response of a Rough Interface. *Phys. Rev. B* **1986**, *34*, 4870–4873. [CrossRef] [PubMed]
65. Liu, S.; Kaplan, T.; Gray, L. Ac Response of Fractal Interfaces. *Solid State Ion.* **1986**, *18–19*, 65–71. [CrossRef]
66. Nyikos, L.; Pajkossy, T. Diffusion to Fractal Surfaces. *Electrochim. Acta* **1986**, *31*, 1347–1350. [CrossRef]
67. Pajkossy, T.; Nyikos, L. Impedance of Fractal Blocking Electrodes. *J. Electrochem. Soc.* **1986**, *133*, 2061–2064. [CrossRef]
68. Nyikos, L.; Pajkossy, T.; Martemyanov, S. Diffusion to a Rotating-Disk Electrode with Fractal Surface. *Sov. Electrochem.* **1989**, *25*, 1381–1384.
69. Nyikos, L.; Pajkossy, T. Electrochemistry at Fractal Electrodes. In *Proceedings of the Instationary Processes and Dynamic Experimental Methods in Catalysis, Electrochemistry and Corrosion*; Sandstede, G., Kreysa, G., Eds.; V C H Verlagsgesellschaft: Weinheim, Germany, 1989; Vol. 120, pp. 361–371.
70. Pajkossy, T.; Nyikos, L. Diffusion to Fractal Surfaces—II. Verification of Theory. *Electrochim. Acta* **1989**, *34*, 171–179. [CrossRef]
71. Pajkossy, T.; Borosy, A.; Imre, A.; Martemyanov, S.; Nagy, G.; Schiller, R.; Nyikos, L. Diffusion Kinetics at Fractal Electrodes. *J. Electroanal. Chem.* **1994**, *366*, 69–73. [CrossRef]
72. Gouyet, J.; Rosso, M.; Sapoval, B. Fractal Structure of Diffusion and Invasion Fronts in 3-Dimensional Lattices Through the Gradient Percolation Approach. *Phys. Rev. B* **1988**, *37*, 1832–1838. [CrossRef]
73. Rosso, M.; Sapoval, B.; Gouyet, J. Fractal Nature of Diffusion, Invasion and Corrosion Fronts. *Solid State Ion.* **1988**, *26*, 172–173. [CrossRef]
74. Sapoval, B.; Chazalviel, J.; Peyriere, J. Electrical Response of Fractal and Porous Interfaces. *Phys. Rev. A* **1988**, *38*, 5867–5887. [CrossRef] [PubMed]
75. Sapoval, B.; Chazalviel, J.; Peyriere, J. Effective Impedance of a Non-Blocking Fractal Electrode. *Solid State Ion.* **1988**, *28*, 1441–1444. [CrossRef]
76. Maritan, A.; Stella, A.; Toigo, F. Anomalous Warburg Impedance and Universal Surface Magnetic Exponent for Gaussian Models in the Presence of Fractal Boundaries. *Phys. Rev. B* **1989**, *40*, 9269–9273. [CrossRef]
77. Borosy, A.; Nyikos, L.; Pajkossy, T. Diffusion to Fractal Surfaces—V. Quasi-Random Interfaces. *Electrochim. Acta* **1991**, *36*, 163–165. [CrossRef]
78. Arvia, A.; Salvarezza, R. Progress in the Knowledge of Irregular Solid Electrode Surfaces. *Electrochim. Acta* **1994**, *39*, 1481–1494. [CrossRef]
79. Garcia, M.; Gomez, M.; Salvarezza, R.; Arvia, A. Kinetics of Roughness Relaxation at Gold Electrodes. *J. Electrochem. Soc.* **1994**, *141*, 2291–2296. [CrossRef]
80. Galam, S.; Mauger, A. Universal Formulas for Percolation Thresholds. *Phys. Rev. E* **1996**, *53*, 2177–2181. [CrossRef]
81. van der Marck, S.C. sComment on "Universal Formulas for Percolation Thresholds". *Phys. Rev. E* **1997**, *55*, 1228–1229. [CrossRef]
82. Singh, M.B.; Kant, R. Debye–Falkenhagen Dynamics of Electric Double Layer in Presence of Electrode Heterogeneities. *J. Electroanal. Chem.* **2013**, *704*, 197–207. [CrossRef]

83. Jeanmairet, G.; Rotenberg, B.; Salanne, M. Microscopic Simulations of Electrochemical Double-Layer Capacitors. *Chem. Rev.* **2022**, *122*, 10860–10898. [CrossRef] [PubMed]
84. AL-Bazali, T. Insight into Debye Hückel Length (K − 1): Smart Gravimetric and Swelling Techniques Reveals Discrepancy of Diffuse Double Layer Theory at High Ionic Concentrations. *J. Pet. Explor. Prod. Technol.* **2022**, *12*, 461–471. [CrossRef]
85. Córdoba-Torres, P. Relationship between Constant-Phase Element (CPE) Parameters and Physical Properties of Films with a Distributed Resistivity. *Electrochim. Acta* **2017**, *225*, 592–604. [CrossRef]
86. Orazem, M.E.; Frateur, I.; Tribollet, B.; Vivier, V.; Marcelin, S.; Pébère, N.; Bunge, A.L.; White, E.A.; Riemer, D.P.; Musiani, M. Dielectric Properties of Materials Showing Constant-Phase-Element (CPE) Impedance Response. *J. Electrochem. Soc.* **2013**, *160*, C215. [CrossRef]
87. Gharbi, O.; Dizon, A.; Orazem, M.E.; Tran, M.T.T.; Tribollet, B.; Vivier, V. From Frequency Dispersion to Ohmic Impedance: A New Insight on the High-Frequency Impedance Analysis of Electrochemical Systems. *Electrochim. Acta* **2019**, *320*, 134609. [CrossRef]
88. García-Jareño, J.J.; Agrisuelas, J.; Vicente, F. Overview and Recent Advances in Hyphenated Electrochemical Techniques for the Characterization of Electroactive Materials. *Materials* **2023**, *16*, 4226. [CrossRef]